Journal of
Materials Sciences and Applications

JScholar
Fostering Scholarly Communication

Research Article Open Access

Synthesize of Ceo_2 Nanoparticles and Investigation of Antibacterial, Antifungal, Anticancer Activity

Suresh Gopal[1], Baskaran Iruson[1*], Sathyaseelan Balaraman[2*], Senthilnathan Krishnmoorthy[3] and Manikandan Elayaperumal[4]

[1]Department of Physics, Arignar Anna Govt. Arts College, Cheyyar-604407, Tamil Nadu, India
[2]Department of Physics, University College of Engineering Arni (A Constituent College of Anna University Chennai) Arni-632326, Tamil Nadu, India
[3]Department of Physics, VIT University, Vellore-632014, Tamilnadu, India
[4] Department of Physics, Thiruvalluvar University, TVUCAS Campus, Thennangur, 604408, Tamil Nadu , India

[*]**Corresponding authors:** Baskaran Iruson, Department of Physics, Arignar Anna Govt. Arts College, Cheyyar-604407, Tamil Nadu, India, E-mail: bsseelan03@gmail.com
Sathyaseelan Balaraman, Department of Physics, University College of Engineering Arni (A Constituent College of AnnaUniversity Chennai) Arni-632326, Tamil Nadu, India, E-mail: ibk1978@gmail.com

Received Date: December 28, 2021 **Accepted Date:** January 28, 2022 **Published Date:** January 30, 2022

Citation: Suresh Gopal (2022) Synthesize of Ceo_2 Nanoparticles and Investigation of Antibacterial,Antifungal, Anticancer Activity. J Mater sci Appl 5: 1-19

Abstract

The present research investigates the characterization and biological applications such as anti-bacterial, antifungal, the anticancer activity of synthesized CeO_2 nanoparticles (NPs) by using the Microwave irradiation technique. The structural conformation and size distribution of CeO_2 in the nanometer range has been studied by PXRD and TEM analysis. Further, the optical absorption (bandgap) and Functional group CeO_2 NPs were determined by UV-Vis and FTIR respectively. Powder X-ray diffraction (PXRD) spectrum of synthesized CeO_2 NPs was well- matched with JCPDS number 81-0792 which confirms the arrangement of atoms with a body- centered cubic structure along with cell parameters having average crystalline sizes on 49 nm. The CeO_2 NPs sample containing the main elements such as Cerium metal and Oxygen, further astrong bond between cerium metal and oxygen has been confirmed by EDX and FTIR analysis respectively. Besides, the microbial studies, namely, anti-bacterial, anti-fungal and the response in human breast cancer cells exposed to CeO_2 NPs were analyzed with MDA MB 231 by MTT assay.

Keywords: MDA-MB-231; MTT assay; Anti-bacterial; Antifungal

Introduction

The term Nanotechnology is applied to the various concepts such as fabrication, characterization, explored comprehensively for multifunctional behavior and technological application of nanomaterial's sized and more overplay an important role in controlling the size shape of the properties of the material. Since fabricated nanomaterials have enormous uses in many fields [1-5] worldwide, due to their unique size and shape [6,7], this allows the large development in the Nanotechnological world.

Commercially a large volume of CeO_2 NPs are fabricated because they act as a cracking catalyst in petroleum products, flash memory in electronic devices, gas leakage detecting sensors, polishing chemicals to polish mirrors in many electronic devices and wafers, andadditive fuel cells in diesel to increase combustion efficiency or mileage ((HEI, 2001; Park et al.,2008a). Since CeO_2 NP donates or stores oxygen which is based on the ecological system. If the environment is rich with oxygen, then CeO_2 itself acts as a catalyst but in the case of hydrocarbon combustions, it donates oxygen.

Among the many metal oxide NPs, the synthesized CeO_2 provides beneficial properties such as attractive morphology, highly reactive and strongly oxidizing agents. Since nanoparticlescan bind with the animal's cancer cell line, further these bindings prevent the growth of cancer cells and therefore nanoparticles have the major application of cancer prevention in the biological field [12-14]. The abnormal growth of cancer cells easily spreads to other parts of the body causing damage to organs for cancer patients. The available chemotherapeutic agents may provide the side effects and therefore it is necessary to prepare bio-compatible compounds in the place of drugs to cure cancer disease and further the cost of treatment should be less possible for cancer patients to cure cancer cells and to achieve these benefits, the nanoparticles have been introduced in this recent decade which provides the effective treatment for cancer patients. In this research, we show that the prepared CeO_2 NP is successfully active against the MDA-MB- 231 cell line[15-16]. Further, in this research, the important biological application such as the effective antimicrobial activity using the synthesized CeO_2 has been studied.

Experimental

Preparation of Cerium Oxide (CeO_2) Nanoparticles

The Microwave irradiation technique was employed to synthesize CeO_2NPs. All reactants were purchased from Sigma Aldrich. The precursors used were 1g of Cerium (III) nitrate hexahydrate and 2 g Urea are added in 50 ml of distilled water along with AR grade CeO_2NPs and mixed well; these powders are converted to disk-shaped pellets with the help of a hydraulic handheld and then this pallet sample was kept at 800°C for 30 minutes in a microwave generating furnace. This heating process on the pellet sample which contains CeO_2NPs allows for the reduction of CeO_2NPs. After half an hour of the heating process, the pellet sample (containing CeO_2NPs) has been burnout to finish the process. These samples were ground for 1hrin an agate mortar to make it into fine powder possessing uniform particle size. The obtained material was subjected to different characterization to confirm the appropriateness of device application.

Characterizations techniques

Characterizing the CeO_2 NPs is very essential which provides the structural information (shape, diameter, and average size CeO_2) and many other various predictions such as absorption (or emission) spectrum, bandgap, and functional groups of synthesized CeO_2 NP sample. These various aspects of information can be obtained by using various instruments such as X-ray, UV- Vis spectrometer, FTIR, PL, EDX, and TEM. Among many instruments, TEM alone uses the beam of the electron, to reveal the surface morphological information of the CeO_2 NP sample. Except for TEM, other all instruments use a particular range of electromagnetic radiation to reveal the crystalline nature of the system, CeO_2 NP size, bandgap and functional groups, and thepresence of chemical elements in the CeO_2 NPs.

Test Microorganisms

Aspergillus Mucor fungi was used for carrying out the antimicrobial activity studies. These microorganisms were grown for 3 days at 37 °C in Actinomyces Isolation Media (AIM) broth (Himedia, Mumbai, India). The sensitivity of these microorganisms to the reference antibiotics was checked using mycostatin as a positive control.

Antifungal Activity of the Sample

The samples of iron oxide, erbium oxide and iron oxide/erbium oxide nanoparticles were loaded on Potato Dextrose agar plates at three different volumes (10, 20, and 30 µl) and swabbed with fungi such as Aspergillus and Mucor. Antifungal activities of the samples were determined by well diffusion method on Potato Dextrose Agar (PDA) medium [17]. The PDA medium was composed of (gl^{-1}) potato infusion-200, dextrose -20, and agar-15. The PDA medium waspoured into the Petriplate; and after solidification, the inoculum was spread on the PDA plates with sterile swab moistened with the fungal suspension. All the plates were incubated at 37 °C for 3 days and finally the inhibition zone was analysed. These fungi were grown in Actinomyces Isolation Media (AIM) broth (HIMEDIA Mumbai). Mycostain was used as the positive controlto check the sensitivity against antibiotics by the well diffusion method on PDA medium.

Antibacterial Activity of the Sample

The antibacterial activity of iron oxide, erbium oxide and iron oxide/erbium oxide nanoparticles were tested against Escherichia coli, and Bacillus sp using disc diffusion method. The iron oxide, erbium oxide and iron oxide/erbium oxide nanoparticles were prepared inappropriate concentration of 1 mg/ml with dimethylsulfoxide solution for this process. Then, the dispersed nanoparticles were impregnated to each sterile disc by using micropipette. After thatthe discs were kept on culture swapped Mueller Hinton Agar medium using sterile force and allowed to incubate for 24 hrs. The average zone of inhibition diameter was measured inmillimeter (mm).

Cell Culture and Cell Line Maintenance

The human breast cancer cell lines MDA MB-231 were obtained. Then, these cell lines were grown as a monolayer in Dulbecco's modified Eagle's medium (DMEM: Hi Media Laboratories, Mumbai, India), which was supplemented with 10% fetal bovine serum, 100 U/mLpenicillin, and 100 µg/mL streptomycin (Hi Media Laboratories Mumbai, India) cells grown at 37˚C in incubator under 5% CO_2 with high humidity [18-19].

MTT Assay Method for Evaluation of Cell Viability and Cytotoxicity

The anticancer activity of samples on human breast cancer cell lines MDA MB-231 was determined by the MTT (3-(4, 5-dimethyl thiazol-2yl)-2, 5-diphenyl tetrazolium bromide) assay [20-21]. These cells (1 × 105/well) were plated in 0.2 ml of the cells with concentration of 1 × 105 cells/ml. The plates were incubated for 24 hrs in 5% CO_2 incubator for cytotoxicity. After incubation, normal breast (MDA MB-231) cells were cultured in 1:1 mixture of dimethyl sulfoxide (DMSO). Then, they were added to each well and mixed well by micropipette [22]. The percentage of viable cells was visualized by the development of purple color due to the formation of formazan crystals. The suspension was transferred to the cuvette of a spectrophotometer and observed significant variance/instability in the optical density (OD).Measurements were performed and the concentration required for a 50% inhibition of viability (IC_{50}) was determined and used for the bioassays.

Results and Discussion

PXRD of Cerium oxide (CeO_2) metal oxide nanoparticle:

The PXRD pattern of CeO_2 NPs, thus contains the particle size information and crystalline nature, which was synthesized by Microwave irradiation technique were present in Figure 1a. The peaks in fig.1a are assigned to the cubic structure of CeO_2 with lattice pointsa=b=c=5.412 Å and matched with the JCPDS No. 81-7092. Using Debye - Scherer's formula, the average CeO_2 crystallite size is found as 49 nm[23]. Several Bragg reflections with 2θ valuesof 28.5°, 33°, 47.5°, and 56.4° are observed corresponding to (111), (200), (220), (311), (222) and (422) (Figure 1).. Further, the crystallinity nature, particle size distribution, and phase formation have been confirmed by HRTEM.

TEM

The electrons passing in a TEM instrument through the potential barrier of the synthesized sample afford the topography [Lin P-C 2014, Hinterdorfer P 2011] information of the CeO_2 NPs. In fig.2 (TEM image) can be observed from CeO_2 NPs structured size between 45.112 to 48.556 nm which gives an average crystallite of 46.8 nm (Table 2), and further these crystalline nature [24-25] of the CeO_2 NPs has been confirmed by SsAED pattern (Figure 2d). The results from the TEM image are agreed with the result of XRD data having crystal planes (111) and (200).

EDX Analysis

EDX analysis of CeO_2 NPs was shown in Figure 3, which confirms that the major chemical element such as Cerium and oxygen were present with strong absorption range and homogeneous distributions, further this spectrum proves that the cerium atom uniformly combined with the element oxygen which is summarized in Table.3.

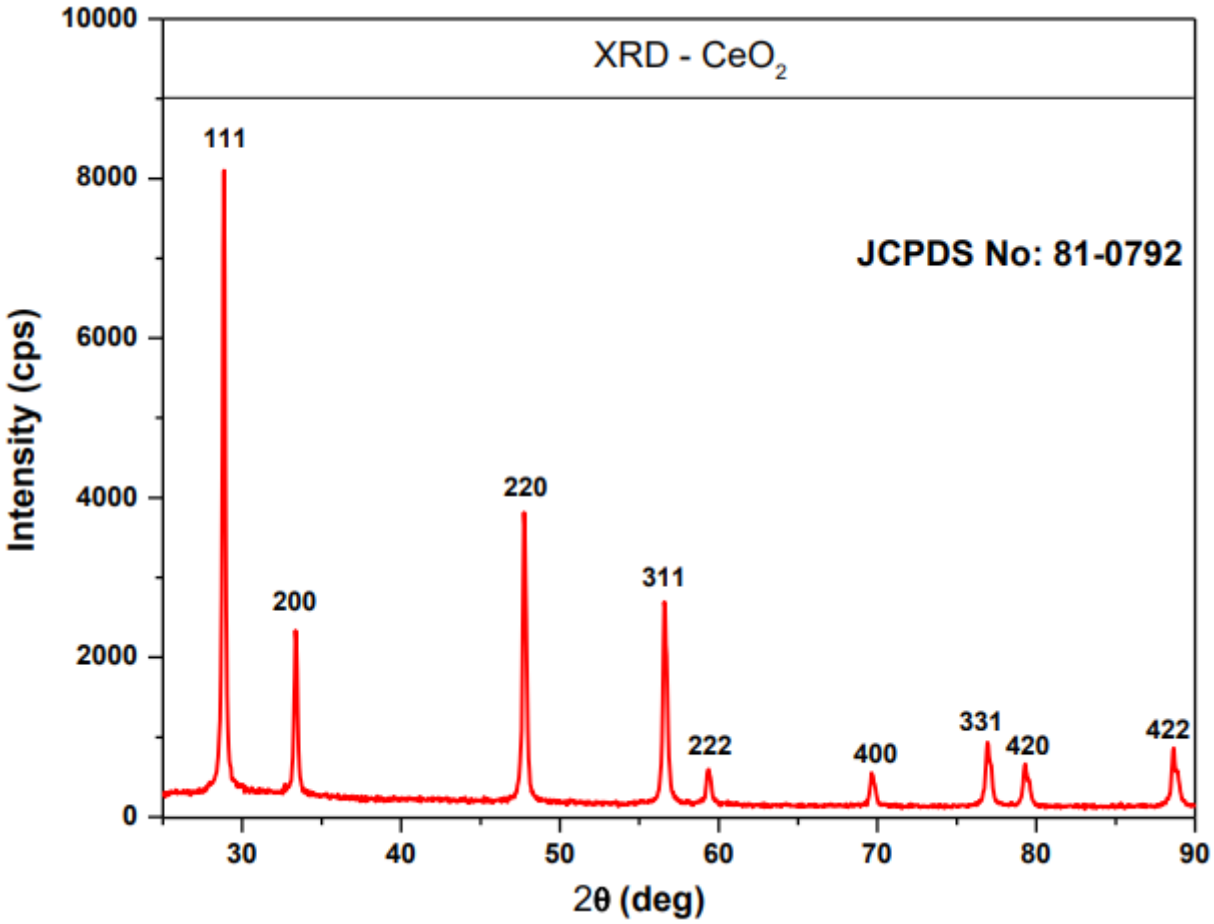

Figure 1: The PXRD pattern of CeO_2 Nanoparticles

Table 1: The deduced magnetic parameters for $CoCe_xFe_{2-x}O_4$ ($0.0 \leq x \leq 0.10$) samples obtained from the M-H loops at 100 K

Samples		Cellparameters (Å)	d space(Å)	Volume (Å)³	Crystalline size (nm)	Structure	
C1		5.4	1.759	158	49.1	FCC	
samples	JCPDS CardNo.	D-Spacing (Å)		Cell Parameters (Å)		Cell Volume (Å)³	
		Calculations	JCPDS	Calculations	JCPDS	Calculations	JCPDS
CeO_2	81-0792	1.7596	1.7609	5.408	5.412	158.34	158.55

FTIR

FTIR spectrum of CeO_2 NP is shown in Figure 4. The band at 425 cm^{-1} shows the presence of metal oxide, thus predicts the presence of a strong bond and stretching between metal cerium andoxygen (i.e. O-Ce-O) [26]. The major peak at the point of 706 cm-1 corresponds to the stretching vibration of doubly coordinated oxygen due to corner shared element oxygen to two cerium atoms. The peak at the point of 1466 cm-1 is assigned to the C-N stretching vibration of urea which was added in the synthesis process. The peaks at the point of 1467 and 3428 cm-1 correspond to stretching vibration of c=c and O-H respectively.

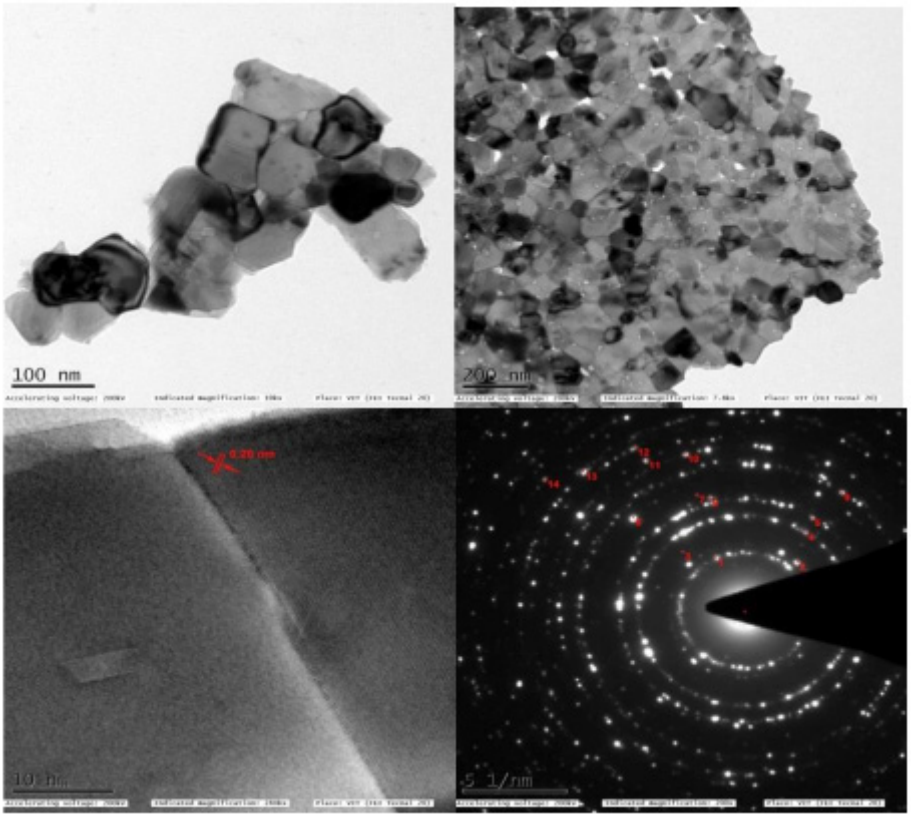

Figure 2: TEM images of Cerium Oxide (CeO_2) Nanoparticles

Table 2: The size distributions of CeO_2 NPs

Area (nm)	Mean (nm)	Min (nm)	Max (nm)
48.556	86.527	10.288	251
47.663	71.1	26.583	253.647
46.005	85.089	21.012	145
45.112	79.468	16.884	121
Average = 46.8 nm			

UV-Vis spectroscopy

UV-Vis affords the bandgap as well as the stability of the CeO_2 NPs. The UV-Vis of CeO_2 NPs is present in fig. 5a and 5b. The optical property of CeO_2 NP allows them to absorb with a particular range of wavelengths of UV-Vis radiations and maximum absorption and cut- off wavelengths were found at 270 nm and 430 nm respectively. In Figure 5c, it was observed that the bandgap energy of CeO_2 NPs be around 3eV. This shows that the synthesized CeO_2 NPs could be useful in few medical applications [27,28].

Photoluminescence (PL) spectroscop

PL spectrum of CeO_2 is useful to detect the high-quality crystalline nature and the fine structure of the sample. PL at ambient room temperature was implemented to reveal the optical absorption of Cerium Oxide (CeO_2) nanoparticles. In Figure 6, CeO_2 NP shows the UV emissionand green excitations at 284 nm and 550 nm respectively. These results were also reported in previous research [29]. In common, the presence of oxygen

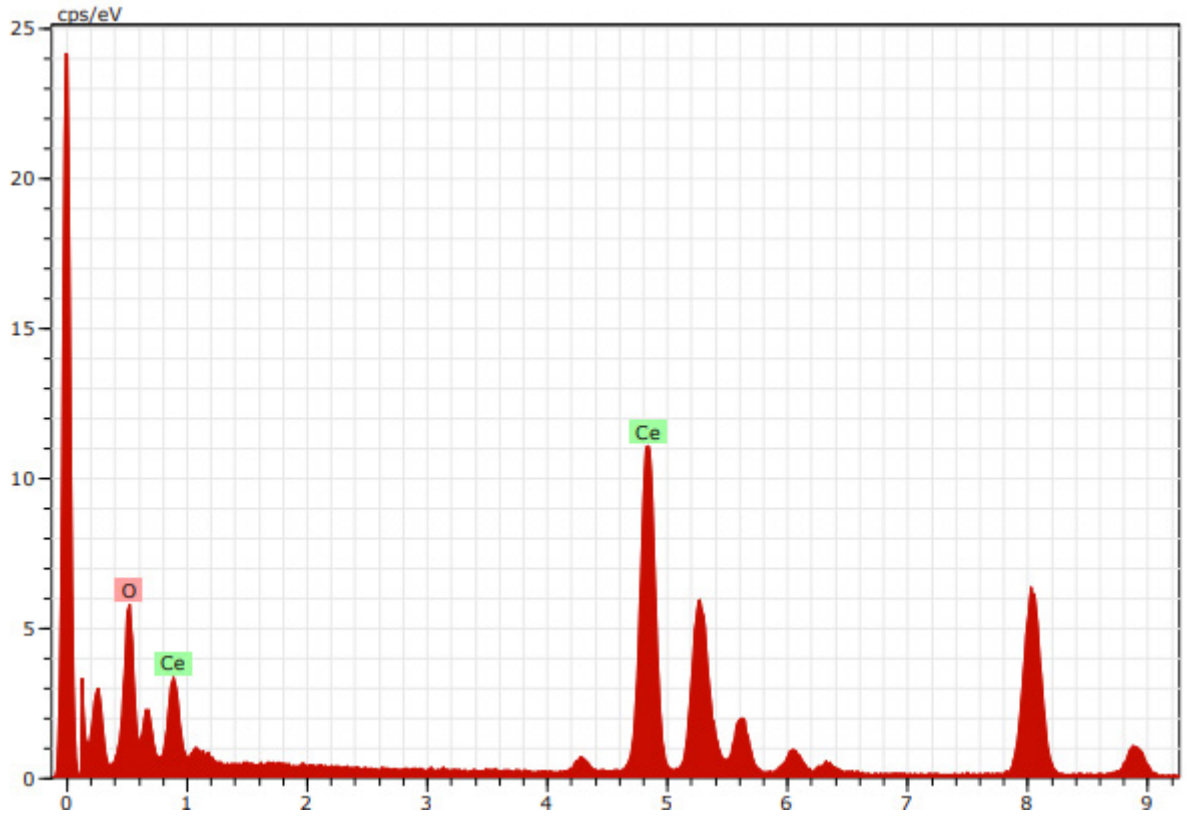

Figure 3: The EDX pattern of CeO_2 Nanoparticles

Table 3: The percentage of chemical elements in the synthesized CeO_2.NPs sample

Spectrum: Spectrum 525-Ce						
Element Series		Net	unn. C (% .Wt)	Norm. C (% .Wt)	Atom. C (% .at)	Error (% .Sigma) (Wt 3)
Cerium	L-series	94064	89.31	89.31	48.83	26.90
Oxygen	K-series	13405	10.69	10.69	51.17	1.08
Total:	**100.00**	**100.00**	**100.00**			

vacancies in the sample creates defects, thus are responsible for the creation of broad peaks at larger wavelengths of light.

Anti-Fungal activity

The synthesized metal CeO_2 NPs provides fewer hazards to the outside environment, but its toxic activity against the various fungi is higher [30-32], to find out the antifungal activity of CeO2 NPs, the disc diffusion technique has been carried out and results are shown in fig.7 and further summarized in Table 5.

The cell viability effect (or zone inhibition) of CeO_2 nanoparticles on the fungi is discussed by explaining the two

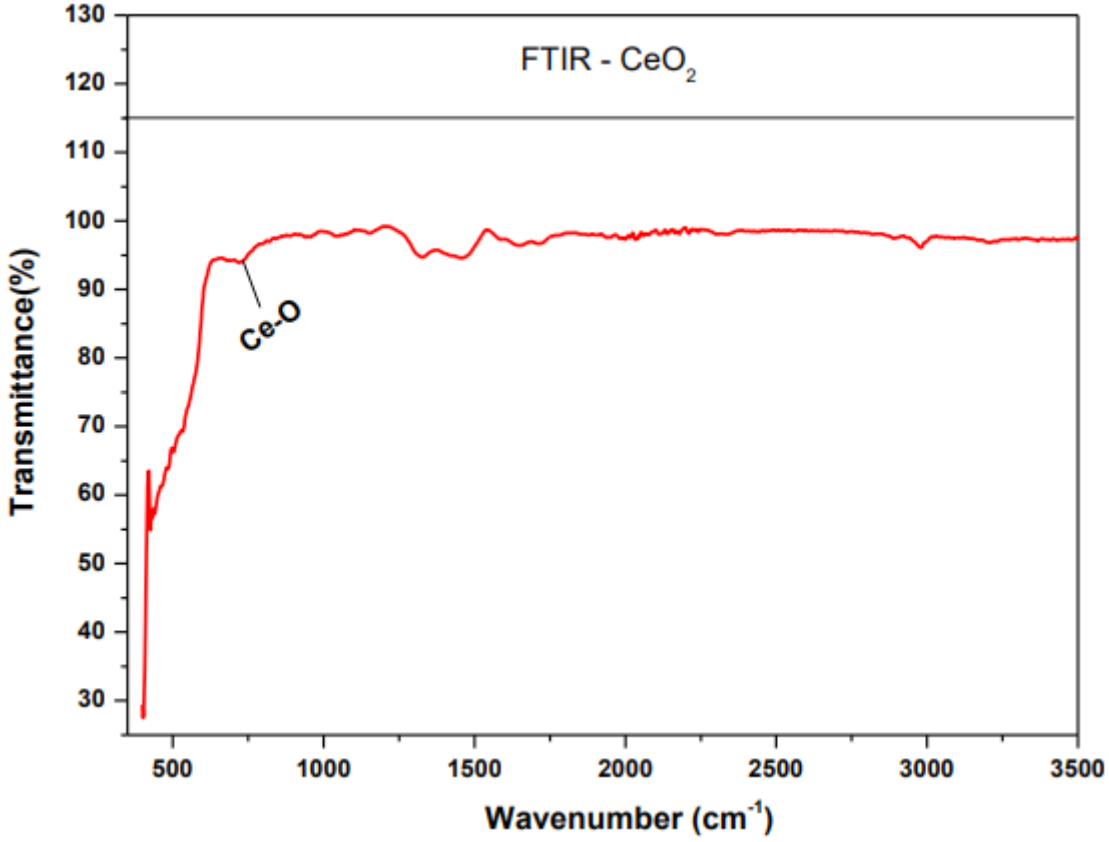

Figure 4: FTIR spectrum of Cerium Oxide (CeO_2)

Table 4: The peak positions and corresponding functional groups of synthesized CeO_2 NPs

Observed Band Position $(cm)^{-1}$	**Assignments**
1311	C-N Stretching vibration
1647	C=C Stretching vibration
3428	O-H Stretching vibration
425, 706	Cerium Oxide

different mechanisms. First, the creation of H_2O_2 around the CeO_2 NP leads to the possible hydrogen bond development between (OH group) cellulose content of fungi and oxygen atom which causes higher zone inhibition. In second, the release of Ce^{2+} ion causes damage to the cell membrane which leads to the growth of higher zone inhibition [34-45]. Results reveal that 300 mg of the CeO_2 NP sample provides a higher toxic activity than the toxic activity provided by the lower concentrations of CeO_2 NPs. The separate 300 mg of the CeO_2 NPs causes the higher zone inhibition as 20 mm and 15 mm respectively for *Mucor* and *Aspergillus*. Finally, the results from figure 7 show that the toxicity given by the CeO_2 is higher for *Mucor* than *Aspergillus*.

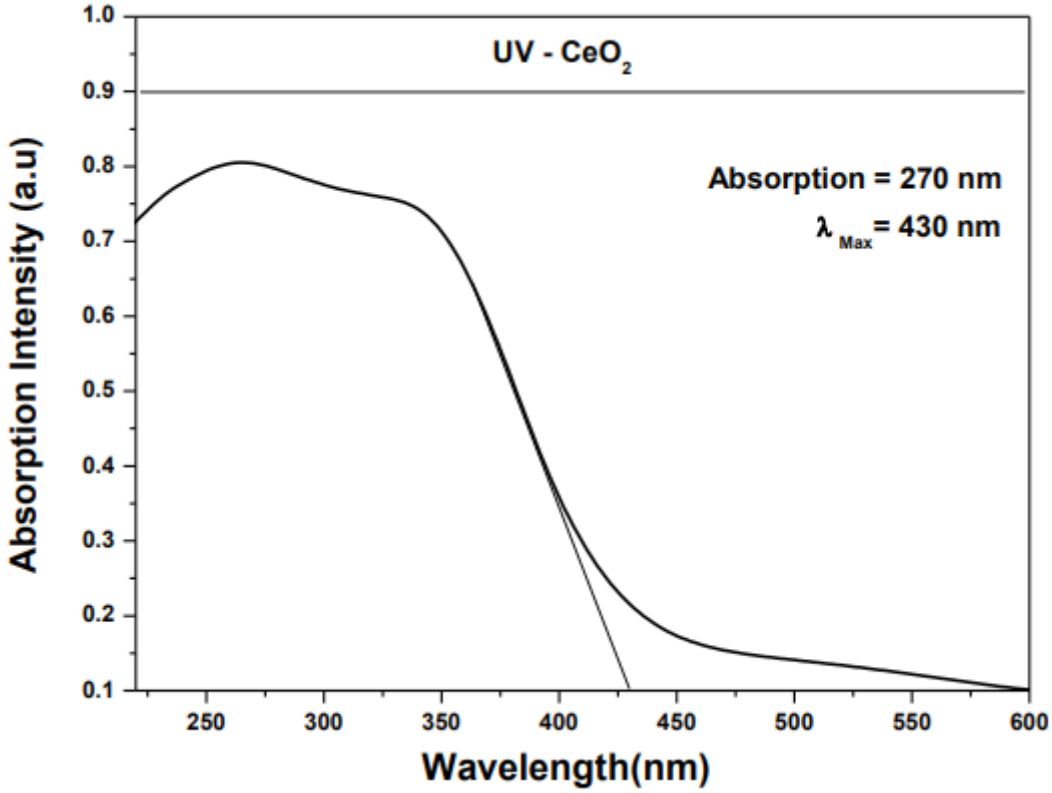

Figure 5a: UV-Vis absorbance spectra of CeO_2 NPs

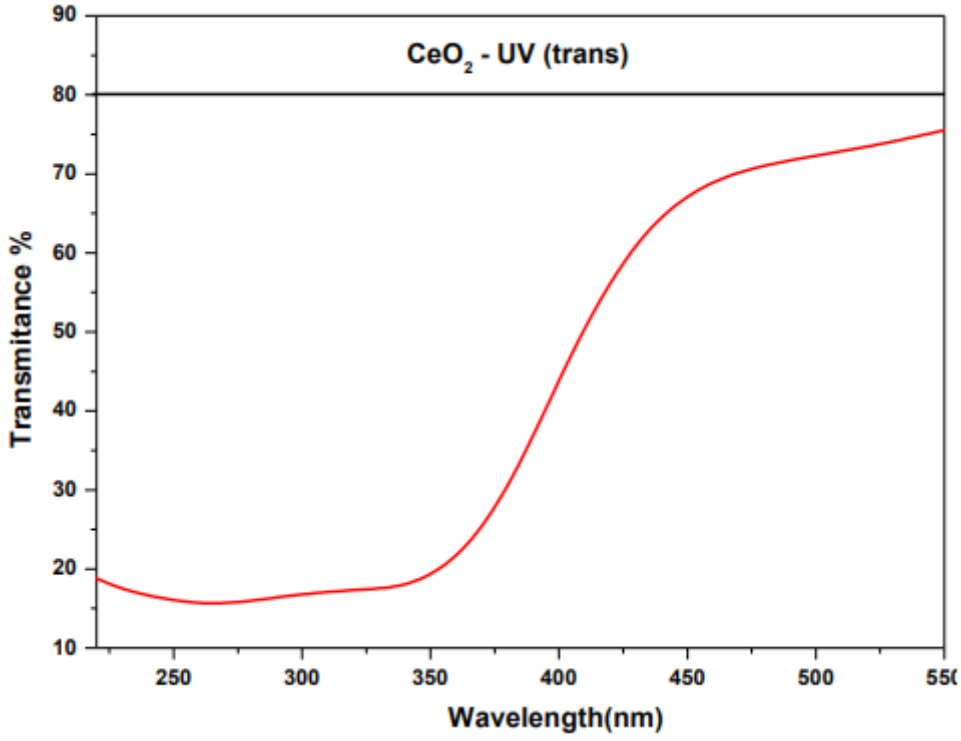

Figure 5b: UV-Vis transmittance spectra of CeO_2 NPs

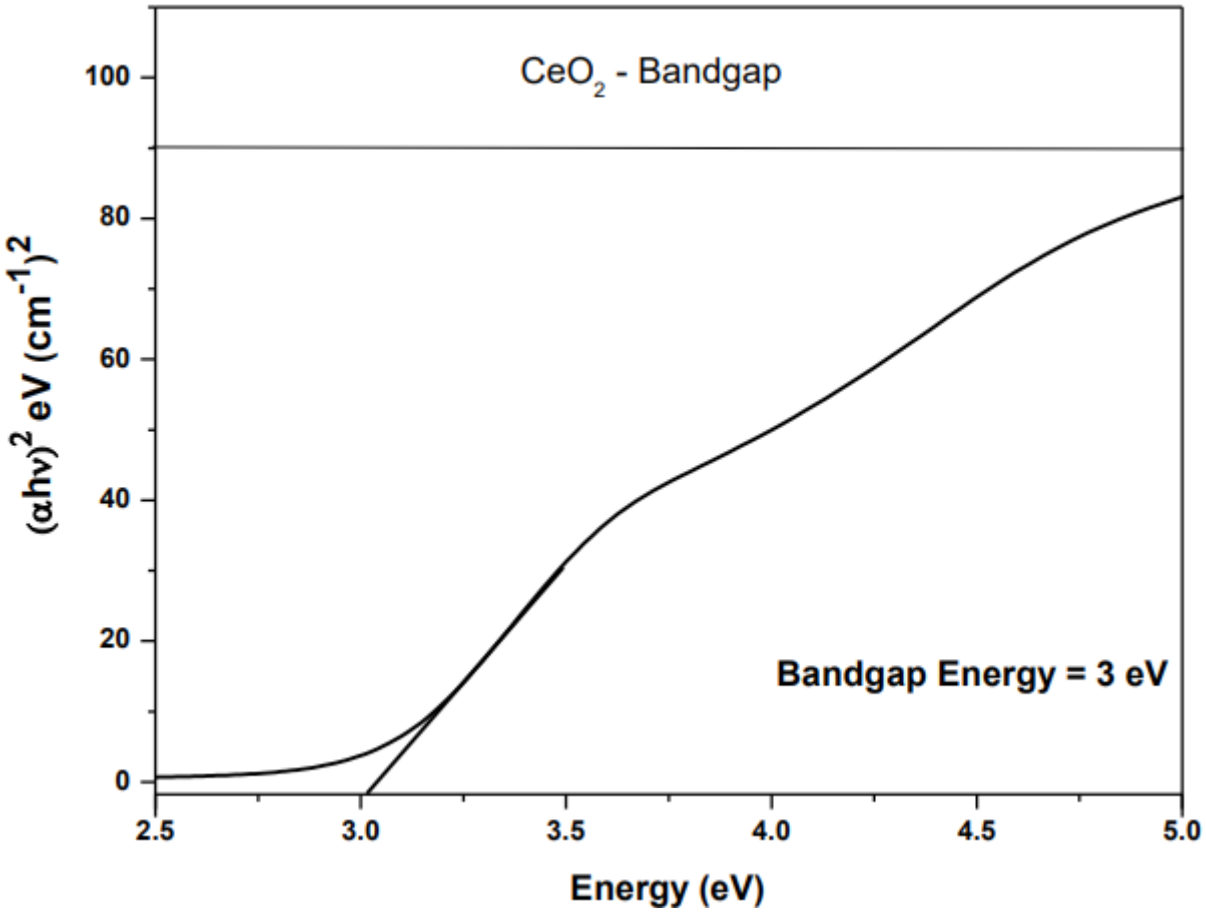

Figure 5c: Photon energy vs. $(\alpha h\nu)^2$ spectrum of CeO_2 NPs

Figure 7 the Anti-fungal activity of Crium oxide nanoparticles. 1) *Aspergillus* and 2) *Mucor* at 100 mg, 200 mg, and 300 mg, 3) concentration where the control.

Anti-cancer

The cytotoxicity of CeO_2 NPs with various concentrations (5 µg, 10 µg, 50 µg, 75 µg, and100 µg /mL) against MDA-MB- 231 cell lines were investigated by the MTT method and its results were present in fig.9, further, the observed values are tabulated (Table 7). In the MTT assay, the cell morphology was captured after 48 hours to obtain the best results. In previous research, the significant results against MDA-MB-231 were observed by adding the 50 µg/mL or 75 µg/mL [52-55]. An advantage of CeO_2 NP is its available lesser size in the sample, so we believed that the synthesized lesser concentrations of CeO_2 NPs in this research, have the higher potential to destroy the MDA-MB-231 cell line. Therefore the chosen concentration of CeO_2 NPsin this research is lesser than the previously published results of the cytotoxicity study. The chosen lowest concentration (5 µg/ml) of CeO_2 NP provided the highest cell destruction with 86% cytotoxicity causing the lesser cell viability (14%.) of the MDA-MB-231 cell line.

Conclusion

In this study, using Microwave radiation the CeO_2 NPs have been prepared and its effective anticancer and antimicrobial studies were successfully executed. The formed CeO_2 crystalline structure and its size range around 45 to 49 nm have been analyzed using XRD and TEM analysis. All the possible major elements and functional groups present in the sample which was synthesized by adding cerium nitrate, urea, and water molecules, have been successfully found using EDX and FTIR studies respectively. The bond between major element cerium and oxygen was identified by noting the absorbance peak at 706 cm-1 in the FTIR spectrum. Antifungal results show that the CeO_2 NP effectively kills higher the number of Mucor than Aspergillus, further the possible mechanism that causes damage to the fungi by using CeO_2 NP was discussed. The synthesized CeO_2 NPs were also found effective against *BACILLUS SP and E. COLI* bacteria. The results of the MTT assay using the synthesized sample against MDA-MB 231 cell lines indicated the higher percentage of toxicity of CeO_2 NPs. Therefore this study was successfully performed towards biological applications.

Funding

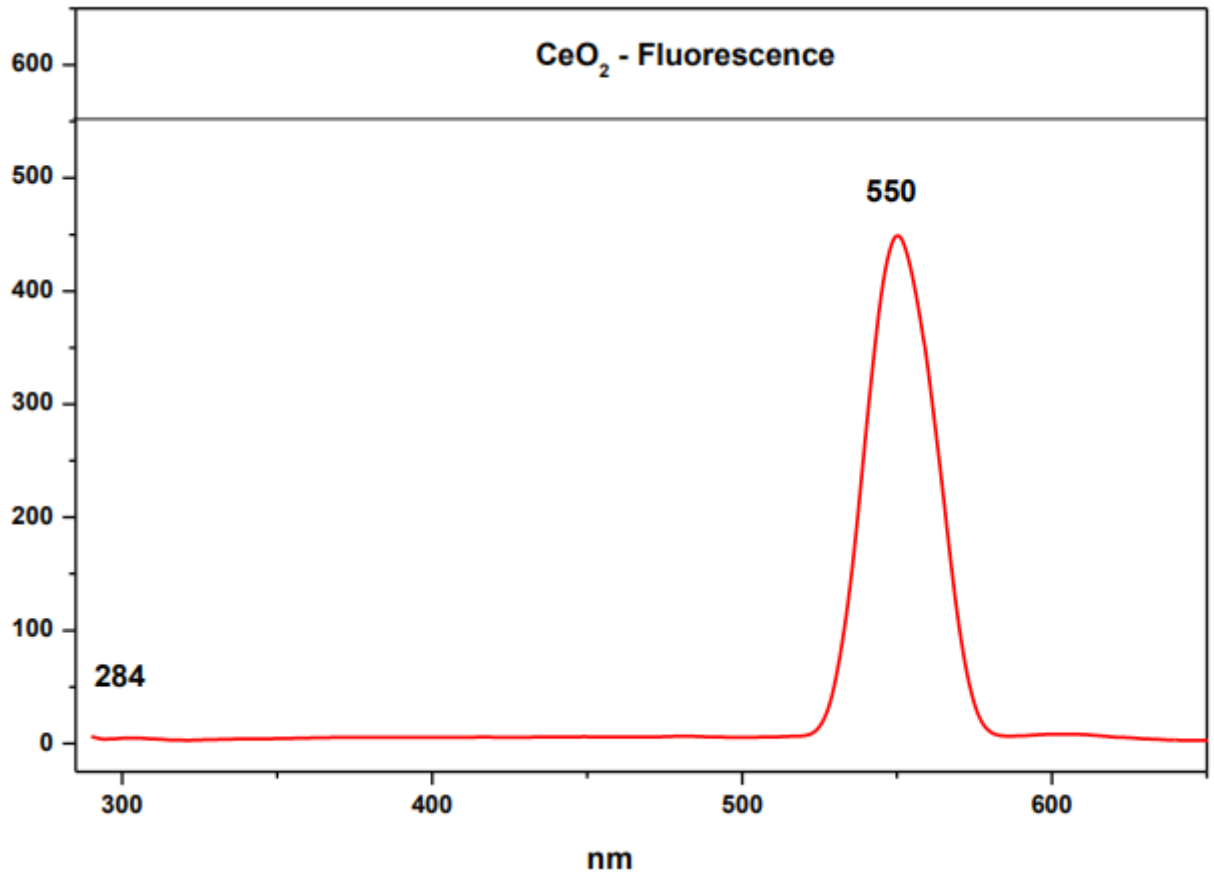

Figure 6: PL spectra of CeO_2 NPs

Table 5: Anti-Bactria of Cerium Oxide (CeO_2)

Nanoparticle	*Aspergilus* % of Zone inhibition			
CeO_2 Nanoparticles	Concentration			Control
	100 mg	200 mg	300 mg	17 mm
	12 mm	13 mm	15 mm	
	Mucor % of Zone inhibition			
	Concentration			Control
	100 mg	200 mg	300 mg	22 mm
	14 mm	18 mm	20 mm	

The technical support of this project has been provided by the Tamilnadu State Council for Science and Technology under grant number, C.No.TNSCST/STP-PRG/AR/2018-2019/9333 is gratefully acknowledged.

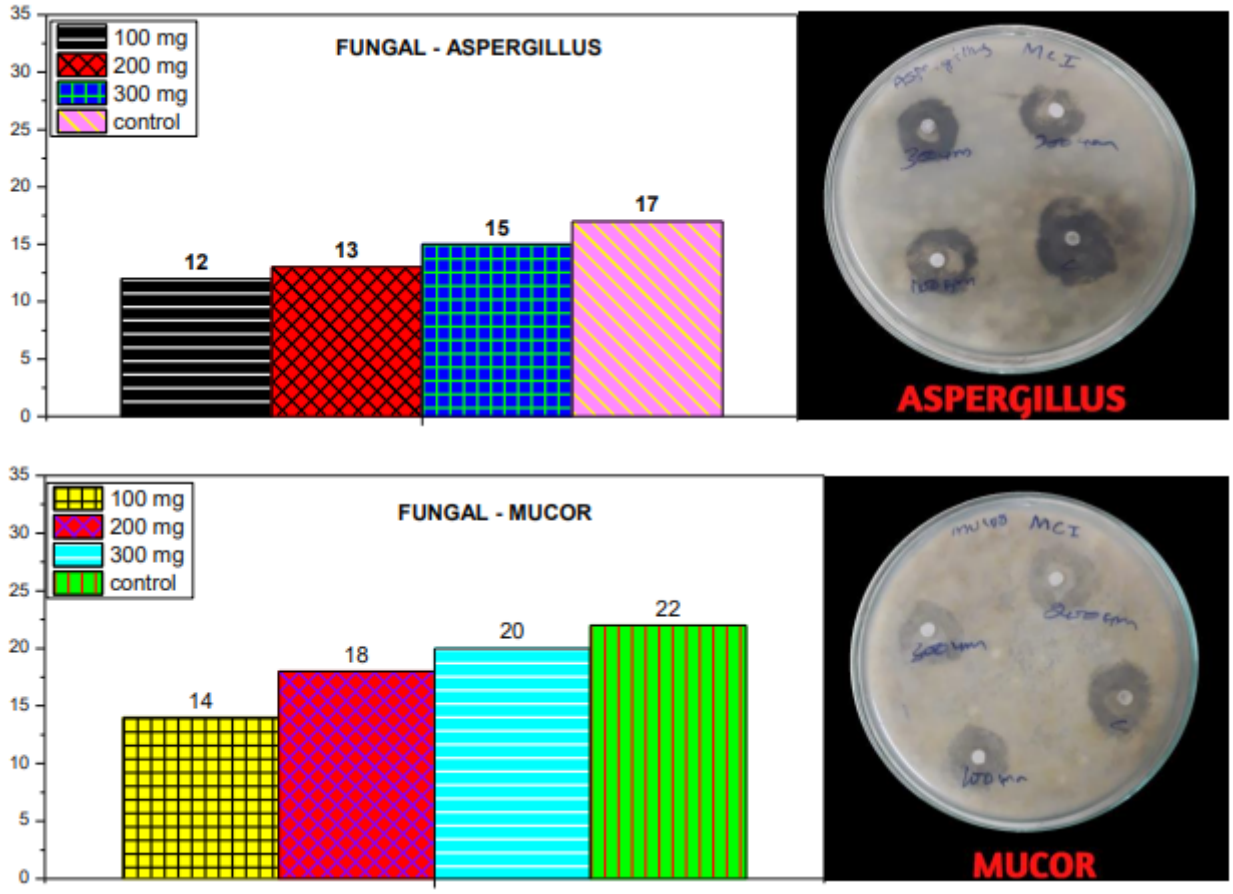

Figure 7: Anti-Fungal activity of Cerium Oxide (CeO)

Table 6: Anti-Bactria of Cerium Oxide (CeO_2)

Nanoparticle	*BACILLUS SP* % of Zone inhibition			
CeO_2 Nanoparticles	Concentration			Control
	100 mg	200 mg	300 mg	19 mm
	14 mm	15 mm	17 mm	
	E. COLI % of Zone inhibition			
	Concentration			Control
	100 mg	200 mg	300 mg	24 mm
	16 mm	20 mm	22 mm	

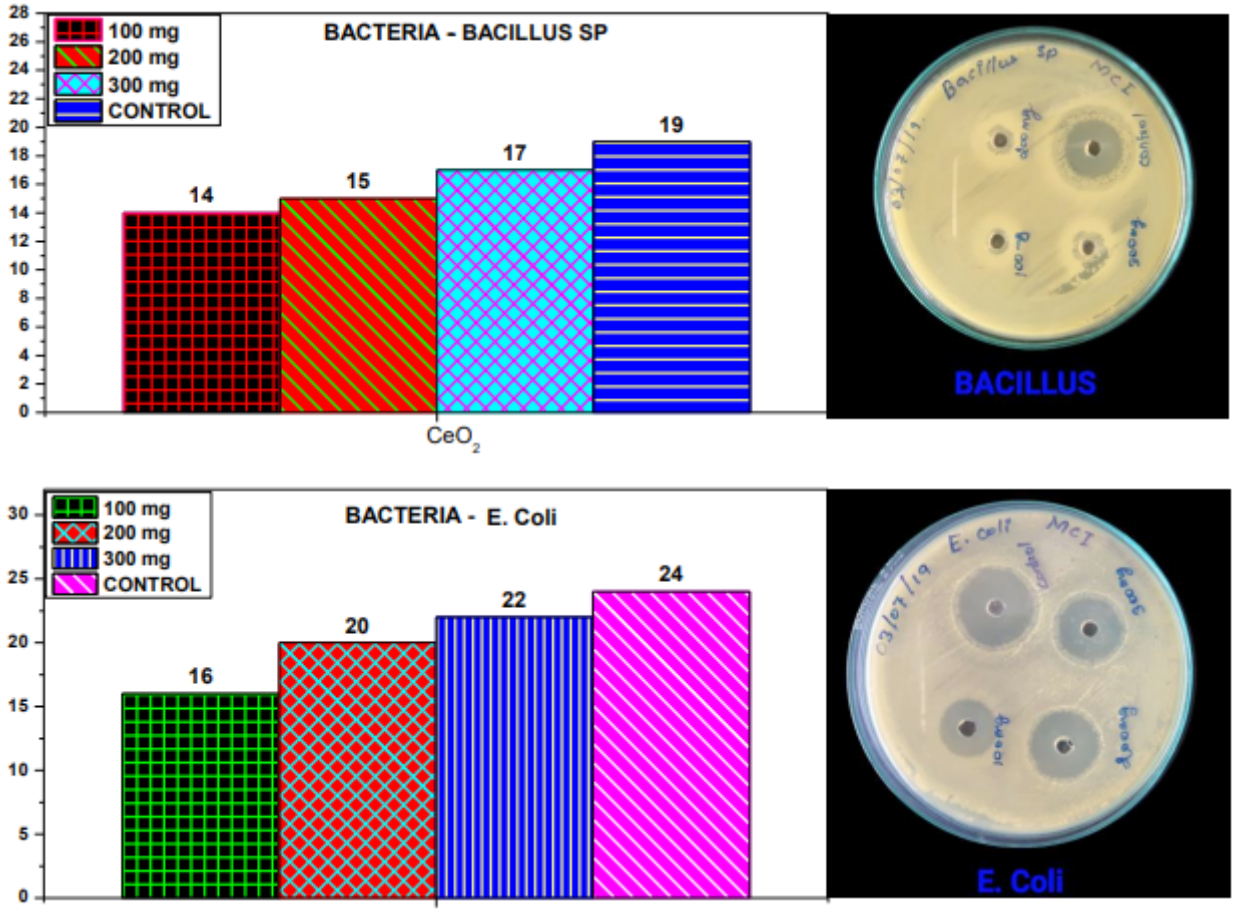

Figure 8: Anti-Bactria of Cerium Oxide (CeO_2)

Table 7: Anti-Bactria of Cerium Oxide (CeO_2).

Sample Particulars		Cytotoxicity(%)	Cell viability(%)	Cytotoxic Re-activity
Description	Conc. (µg)			
C1	5	86	14	Severe
	10	83	17	Severe
	50	76	24	Severe
	75	77	23	Severe
	100	80	20	Severe

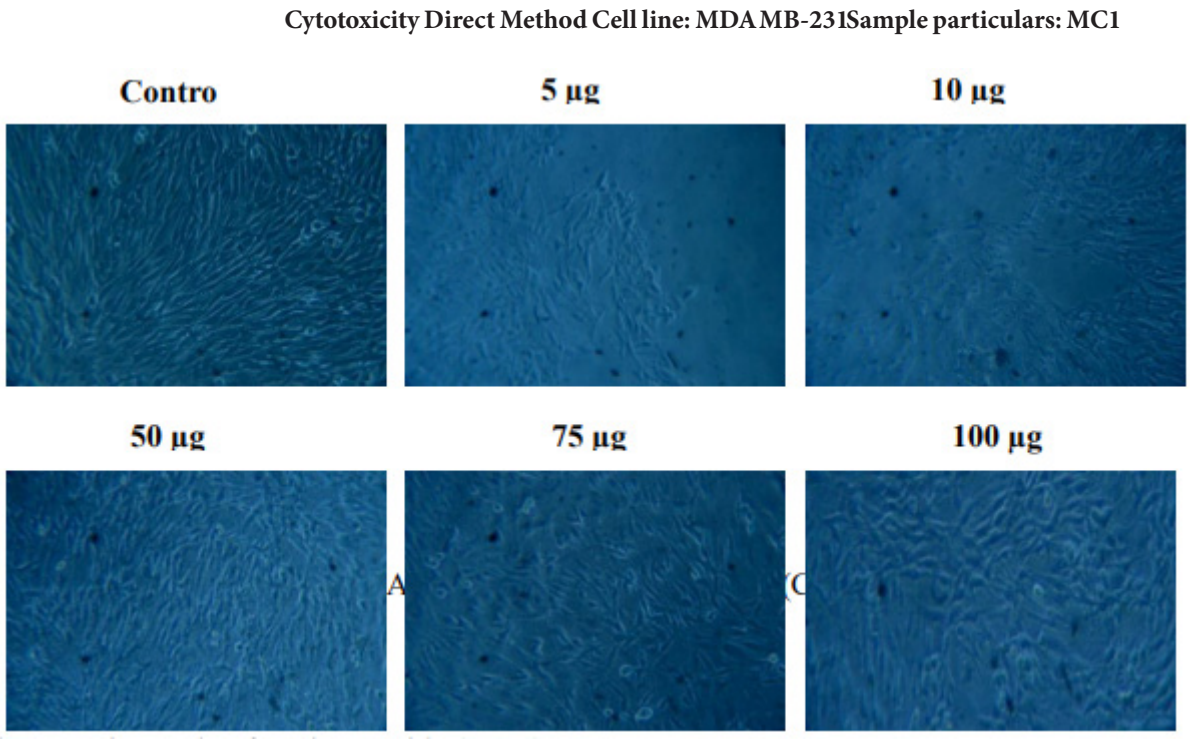

Figure 9: Anti-Bactria of Cerium Oxide (CeO_2).

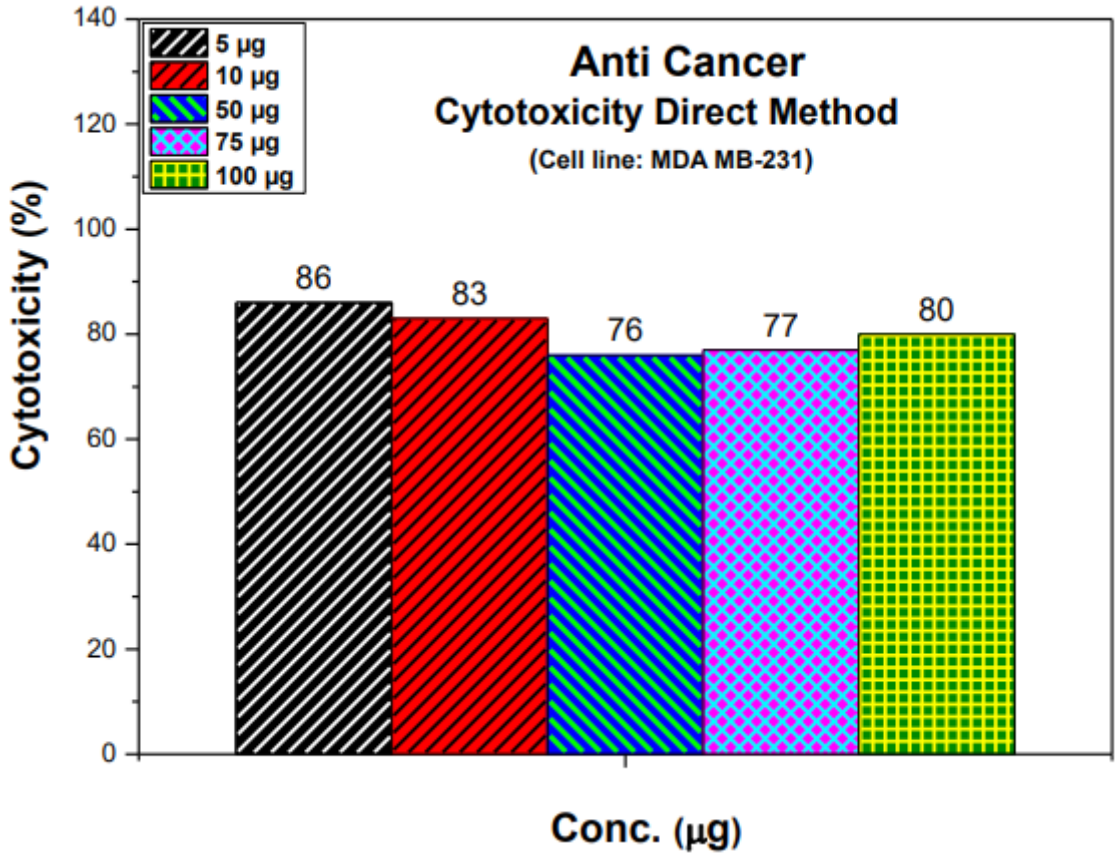

Figure 10: Anti-Bactria of Cerium Oxide (CeO_2)

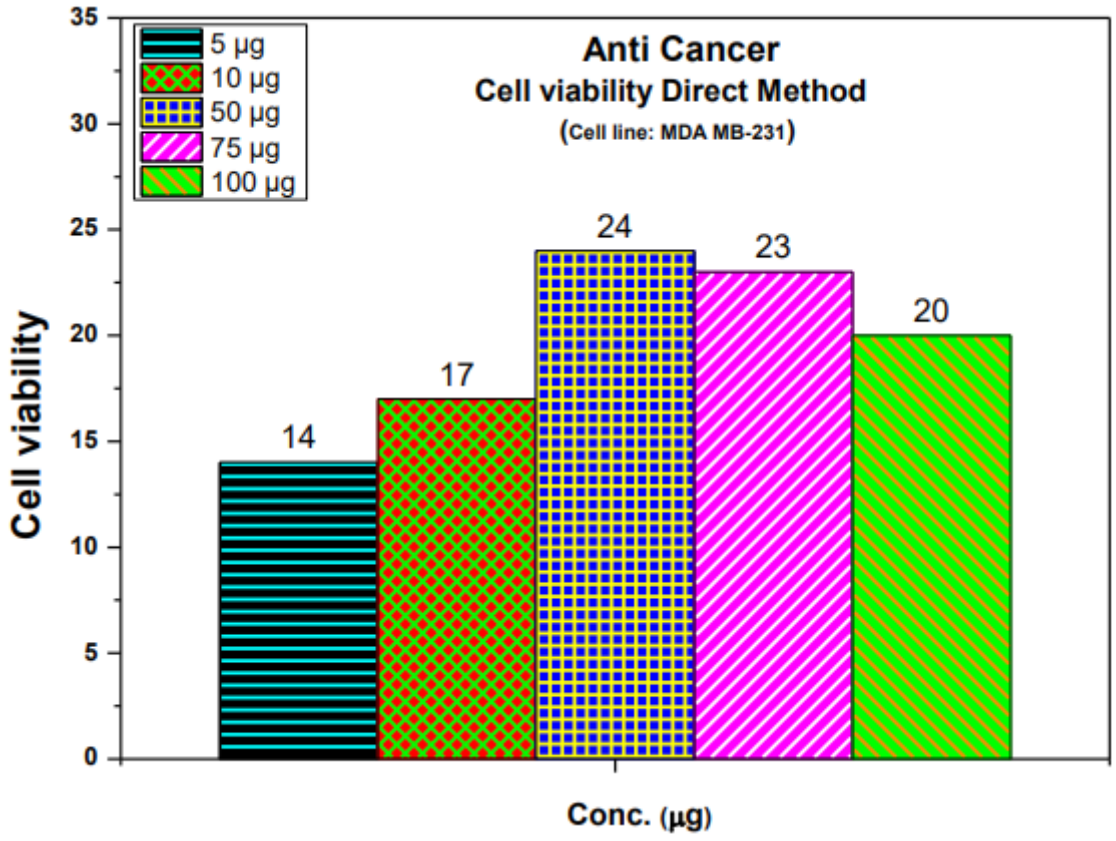

Figure 11: Anti-Bactria of Cerium Oxide (CeO_2)

Conflict Of Interest

The authors declare that they have no conflict of interest

Availability of Data and Material

The authors confirm that the data supporting the findings of this research are available within thearticle and its supplementary materials.

References

1. J Jeevanandam, A Barhoum, YS Chan, A Dufresne, MK Danquah, et al. (2018) Review on nanoparticles and nanostructured materials: history, sources, toxicity and regulations. J Nanotechnol 9: 1050.

2. Sasikala C, Durairaj N, Baskaran I, Sathyaseelan B, Henini M, et al. (2017) Transition metal titanium (Ti) doped LaFeO3 nanoparticles for enhanced optical structural and magnetic properties. Journal of Alloys and Compounds 712: 870-7.

3. C Dipankar, SJC Murugan, SB Biointerfaces, Colloids Surf, B Biointerfaces 2012,

98, 112.

4. Sasikala C, Suresh G, Durairaj N, Baskaran I, Sathyaseelan B, et al. (2020) Influences of Ti4+ ion on dielectric property in perovskite structure of La ferrite (LaFe1-XTiXO3). J Alloys Compounds: 155040.

5. A Hamidi, ME Yazdi, MS Amiri, HA Hosseini, M Darroudi, (2018) Res Chem. Intermed 45: 2915.

6. Sasikala C, Suresh G, Durairaj N, Baskaran I, Sathyaseelan B, et al. (2019) Chemical, Morphological, Structural, Optical, and Magnetic Properties of Transition Metal Titanium (Ti)-Doped LaFeO 3 Nanoparticles. J Superconductivity Novel Magnetism 32: 1791-7.

7. MC Roco (2003) J Nanopart Res 5: 181.

8. Suresh G, Sathishkumar R, Iruson B, Sathyaseelan B, Senthilnathan K, Manikandan E (2019) Study on structural, luminescence properties and Hall Effect of SnO2 nanoparticles obtained by a Co-precipitation technique. Int J Nano Dimension, 10: 242-51.

9. B Nowack, TD Bucheli (2007) Environ. Pollut 150: 5.

10. Aseyd Nezhad S, Es-haghi A, Tabrizi MH (2020) Green synthesis of cerium oxide nanoparticle using Origanum majorana L. leaf extract, its characterization and biological activities. Applied Organometallic Chem 34: e5314.

11. S Teske, C Detweiler (2015) Int J Environ. Res Public Health 12: 1112.

12. Xia Lei, Jian Wu, Baoxuan Huang, Yun Gao, Jia Tian, Weian Zhang (2020) Enhanced photodynamic therapy through supramolecular photosensitizers with an adamantyl- functionalized porphyrin and a cyclodextrin dimer." Chemical Communications 56, no. 75: 11134-7.

13. M Rafique, I Sadaf, MS Rafique, MB Tahir, Artif (2017) Cells Nanomed. Biotechnol 45: 1272.

14. Soosen SM, Bose L, George KC (2009) Optical Properties of ZnO Nanoparticles. SB Academic Review. 2009: 57-65.

15. Eid AM, Hawash M (2021) Biological evaluation of safrole oil and safrole oil nanoemulgel as antioxidant, antidiabetic, antibacterial, antifungal and anticancer. BMC Complementary Medicine and Therapies 21: 1-12.

16. Hawash M (2019) Highlights on Specific Biological Targets; Cyclin-Dependent Kinases, Epidermal Growth Factor Receptors, Ras Protein, and Cancer Stem Cells in Anticancer Drug Development. Drug research.

17. Parkin DM (2001) Global cancer statistics in the year 2000. Lancet Oncol 2: 533-43.

18. Inbathamizh L, Mekalai Ponnu T, Janancy Mary E (2013) In Vitro Evalua-tion of Antioxidant and Anticancer Potential of Morinda pubescens Synthesized Silver Nanoparticles. J Pharmacy Res 6: 32-8.

19. Mosmann T (1983) Rapid Calorimetric Assay for Cellular Growth and Survival: Application to Proliferation and Cytotoxicity Assays. J Immunological Methods 65: 55-63.

20. Krishnaraj C, Jagan EG, Rajasekar S, Selvakumar P, Kalaichelvan PT, et al. (2010) Synthesis of Silver Nanoparticles Using Acalypha indica Leaf Ex-tracts and Its Antibacterial Activity against Water Borne Pathogens. Colloids and Surfaces B: Biointerfaces 76: 50-6.

21. Kroemer G, Zamzami N, Susin SA (1997) Mitochondrial Control of Apoptosis. Immunology Today 18: 44-51.

22. R Bakkiyaraj, G Bharath, K Hasini, Ramsait A, Abdel-Wahab, et al. (2016) Solution combustion synthesis and physico-chemical properties of ultrafine CeO2 nanoparticles and their photocatalytic activity, RSC Adv 6: 51238–45.

23. M Rafique, I Sadaf, MS Rafique, MB Tahir, Artif (2017) Cells

Nanomed. Biotechnol 45: 1272.

24. KS Hemalatha, K Rukmani (2016) Synthesis, characterization and optical properties of polyvinyl alcohol-cerium oxide nanocomposite films, RSC Adv 6: 74354–66.

25. C Xu, X Qu (2014) Cerium oxide nanoparticle: a remarkably versatile rare earth nanomaterial for biological applications, NPG Asia Mater 6: 90.

26. D Wang, Y Kang, V Doan-Nguyen, J Chen, R Kungas, et al. (2011) Synthesis and oxygen storage capacity of two-dimensional ceria nanocrystals, Angewandte Chemie 50: 4378–81.

27. S Brinkman, H Takamura, HL Tuller, T Iijima (2010) The oxygen permeation properties of nanocrystalline CeO2 thin films, J. Electrochem Soc 157: B1852–B1857.

28. V Matolin, M Cabala, I Matolinova, M Skoda, M Vaclavu, et al. (2010) Pt and Sn doped sputtered CeO2 electrodes for fuel cell applications, Fuel Cells 10: 139–44.

29. L Gal, S Abanades (2012) Dopant incorporation in ceria for enhanced water-splitting activity during solar thermochemical hydrogen generation, J. Phys Chem 116: 13516-23.

30. Gurunathan S, Han JW, Eppakayala V, Jeyaraj M, Kim JH (2013) Cytotoxicity of biologically synthesized silver nanoparticles in MDA-MB-231 human breast cancer cells. BioMed research international.

31. Cassee FR, Van Balen EC, Singh C, Green D, Muijser H, et al. (2011) Exposure, health and ecological effects review of engineered nanoscale cerium and cerium oxide associated with its use as a fuel additive. Critical reviews in toxicology 41: 213-29.

32. Chahal S, Kumar A, Kumar P (2020) Erbium-doped oxygen deficient cerium oxide: Bi-functional material in the field of spintronics and photocatalysis. Applied Nanoscience: 1-13.

33. Ravishankar, Thammadihalli Nanjundaiah (2015) Synthesis and characterization of CeO2 nanoparticles via solution combustion method for photocatalytic and antibacterial activity studies." Chemistry Open 4.2 (2015): 146-154.

34. Cassee FR, Van Balen EC, Singh C, Green D, Muijser H, et al. (2011) Exposure, health and ecological effects review of engineered nanoscale cerium and cerium oxide associated with its use as a fuel additive. Critical reviews in toxicology, 41: 213-29.

35. Yu Yang, Sai Xu, Yuefeng Gao, Muhan Jiang, Xiangping Li, et al. (2020) Enhanced photothermal conversion performances with ultra-broad plasmon absorption of Au in Au/Sm2O3 composites." Journal of the American Ceramic Society.

36. S Teske, C Detweiler (2015) Int J Environ Res Public Health 12: 1112.

37. Geiser M, Rothen-Rutishauser B, Kapp N, Schurch S, Kreyling W, et al. (2005) Environ Health Perspect 113: 1555–60.

38. R Bakkiyaraj, G Bharath, K Hasini Ramsait, A Abdel-Wahab, EH Alsharaeh, et al. (2016) Solution combustion synthesis and physico-chemical properties of ultrafine CeO2 nanoparticles and their photocatalytic activity, RSC Adv 6: 51238–45.

39. M Rafique, I Sadaf, MS Rafique, MB Tahir, Artif (2017) Cells Nanomed. Biotechnol 45: 1272.

40. KS Hemalatha, K Rukmani (2016) Synthesis, characterization and optical properties of polyvinyl alcohol-cerium oxide nanocomposite films, RSC Adv 6: 74354–66.

41. Dananjaya SH, Kulatnga DC, Godahewa GI, Nikapitiya C, Oh C, et al. (2017) Preparation, Characterization, and Antimicrobial Properties of Chitosan– Silver Nanocomposites Films Against Fish Pathogenic Bacteria and Fungi. Ind J microbiol 57: 427-37.

42. Fathima AF, Mani RJ, Sakthipandi K, Manimala K, Hossain A (2019) Enhanced Antifungal Activity of Pure and Iron-Doped ZnO Nanoparticles Prepared in the Absence of Reducing Agents. J Inorganic and Organometallic Polymers and Materials. 30: 1-9.

43. Azizi M, Sedaghat S, Tahvildari K, Derakhshi P, Ghaemi A (2017) Synthesis of silver nanoparticles using Peganum harmala extract as a green route. Green Chem Lett Rev 10: 420-7.

44. Ottoni CA, Simões MF, Fernandes S, Dos Santos JG, Da Silva ES, de Souza RFB, et al. (2017) Screening of filamentous fungi for antimicrobial silver nanoparticles synthesis. AMB Express 7: 31.

45. Omidi S, Sedaghat S, Tahvildari K, Derakhshi P, Motiee F (2018) Biosynthesis of silver nanocomposite with Tarragon leaf extract and assessment of antibacterial activity. J Nanostruct Chem 8: 171-8.

46. Wang H, Ma H, Zheng W, An D, Na C (2014) Multifunctional and recollectable carbon nanotube ponytails for water purification. ACS Appl. Mater. Interfaces 6: 9426–34.

47. Musarrat J, Dwivedi S, Singh BR, Al-Khedhairy AA, Azam A,

et al. (2010) Production of antimicrobial silver nanoparticles in water extracts of the fungus Amylomyces rouxii strain KSU-09. Bioresour. Technol 101: 8772–6.

48. Shazia P, Abdul AW, Mohammad AS, Devi HS, Mohd YB, et al. (2017) Preparation, characterization and antifungal activity of iron oxide nanoparticles. Microb Pathog 115: 287-92.

49. Esra B, Umit MS, Cansin S, Serpil E, Omer K (2012) Oxidative stress and antioxidant defense, World Allergy Organ J 5: 9–19.

50. Sudhanshu SB, Jayanta KP, Krishna P, Niladri P, Hrudayanath T (2012) Characterization and evaluation of antibacterial activities of chemically synthesized iron oxide nanoparticles, World J Nano Sci Eng 2: 196–200.

51. K Kaviyarasu, A Mariappan, K Neyvasagam, A Ayeshamariam, P Pandi, et al. (2017) Photocatalytic performance and antimicrobial activities of HAp-TiO2 nanocomposite thin films by sol- gel method, Surfaces and Interfaces 6: 247-55.

52. C Xu, X Qu (2014) Cerium oxide nanoparticle: a remarkably versatile rare earth nanomaterial for biological applications, NPG Asia Mater 6: 90.

53. D Wang, Y Kang, V Doan-Nguyen, J Chen, R Kungas, NL Wieder, RJ Gort, C. B. Murray, Synthesis and oxygen storage capacity of two-dimensional ceria nanocrystals, Angewandte Chemie. 50: 4378–81.

54. S Brinkman, H Takamura, HL Tuller, T Iijima (2010) The oxygen permeation properties of nanocrystalline CeO2 thin films. J Electrochem Soc 157: B1852–7.

55. V Matolin, M Cabala, I Matolinova, M Skoda, M Vaclavu, et al. (2010) Pt and Sn doped sputtered CeO2 electrodes for fuel cell applications, Fuel Cells 10: 139–44.